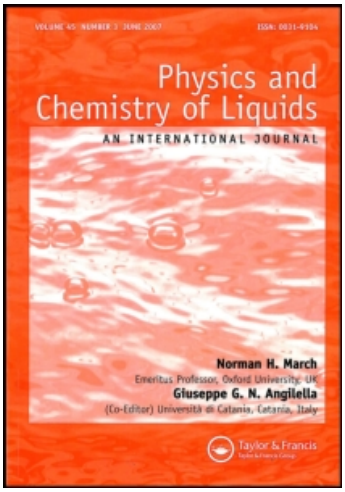

Physics and Chemistry of Liquids
Publication details, including instructions for authors and subscription information:
http://www.informaworld.com/smpp/title~content=t713646857

Exchange energy density and exchange potential via a hartree-fock plus mp2 study of the electron liquid in the ground-state conformer of glycine

Norman H. March[abc]; Michaela Knapp-Mohammady[a]; Christian Van Alsenoy[d]; Sándor Suhai[a]
[a] German Cancer Research Center (DKFZ), Heidelberg, Germany [b] Department of Physics, University of Antwerp, Belgium [c] Oxford University, Oxford, England [d] Department of Chemistry, University of Antwerp, Belgium

To cite this Article March, Norman H. , Knapp-Mohammady, Michaela , Alsenoy, Christian Van and Suhai, Sándor(2008) 'Exchange energy density and exchange potential via a hartree-fock plus mp2 study of the electron liquid in the ground-state conformer of glycine', Physics and Chemistry of Liquids, 46: 3, 242 — 254
To link to this Article: DOI: 10.1080/00319100701713723
URL: http://dx.doi.org/10.1080/00319100701713723

Physics and Chemistry of Liquids
Vol. 46, No. 3, June 2008, 242–254

Taylor & Francis
Taylor & Francis Group

Exchange energy density and exchange potential via a hartree–fock plus mp2 study of the electron liquid in the ground-state conformer of glycine

NORMAN H. MARCH†‡§, MICHAELA KNAPP-MOHAMMADY†, CHRISTIAN VAN ALSENOY¶ and SÁNDOR SUHAI*†

†German Cancer Research Center (DKFZ), Heidelberg, Germany
‡Department of Physics, University of Antwerp, Belgium
§Oxford University, Oxford, England
¶Department of Chemistry, University of Antwerp, Belgium

(*Received in final form 28 September 2007*)

Very recent criticisms of existing exchange-correlation functionals by Wanko *et al*. applied to systems of biological interest have led us to reopen the question of the ground-state conformer of glycine: the simplest amino acid. We immediately show that the global minimum of the Hartree–Fock (HF) ground-state leads to a planar structure of the five non-hydrogenic nuclei, in the non-ionized form NH_2–CH_2–COOH. This is shown to lie lower in energy than the zwitterion structure NHB_3^+–CH_2–COO^-, as required by experiment. Refinement of the nuclear geometry using second-order Møller–Plesset perturbation theory (MP2) is also carried out, and bond lengths are found to accord satisfactorily with experimentally determined values. The ground-state electron density for the MP2 geometry is then redetermined by HF theory and equidensity contours are displayed. The HF first-order density matrix $\gamma(\boldsymbol{r}, \boldsymbol{r}')$ is then used to obtain similar exchange-energy density ($\epsilon_x(\boldsymbol{r})$) contours for the lowest conformer of glycine. At first sight, their shape looks almost the same as for the density $\rho(\boldsymbol{r})$, which seems to vindicate the LDA proportional to $\rho(\boldsymbol{r})^{3/4}$. However, by way of an analytically soluble model for an atomic ion, it is shown that this has to be corrected to obtain an accurate HF exchange energy E_x as the volume integral of $\epsilon_x(\boldsymbol{r})$. Finally, recognizing that for larger amino acids, the use of HF plus MP2 perturbation corrections will become prohibitive, we have used the HF information for $\epsilon_x(\boldsymbol{r})$ and $\rho(\boldsymbol{r})$ to plot the truly non-local exchange potential proposed by Slater, from the density matrix $\gamma(\boldsymbol{r}, \boldsymbol{r}')$. This latter calculation should be practicable for large amino acids, but there adopting Becke's one-parameter form of $\epsilon_x(\boldsymbol{r})$ correcting LDA exchange. Some future directions are suggested.

Keywords: Inhomogeneous electron liquid; Exchange energy and potential; Glycine

1. Introduction

While, in principle, density functional theory (DFT) is a very attractive method to apply to molecules of interest in biology, a serious study by Wanko *et al*. [1] has led them very

*Corresponding author. Tel.: (49) 6221 42 2369. Fax: (49) 6221 42 2333. Email: S.Suhai@dkfz.de

Physics and Chemistry of Liquids
ISSN 0031-9104 print/ISSN 1029-0451 online © 2008 Taylor & Francis
DOI: 10.1080/00319100701713723

recently to strongly warn about the inadequacies of presently used approximate exchange-correlation functionals for such molecular biophysical problems.

Having interests in the simplest amino acids [2], we have therefore re-examined the interesting contributions on gaseous glycine by Stepanian *et al*. [3] and Wang *et al*. [4] both of which studies were directly concerned with three low-lying conformers of the smallest amino acid: glycine.

Because of the approximations to the exchange energy and exchange potential made in the DFT functionals used in references [3] and [4] above, we have returned to Hartree–Fock (HF) theory, which treats 'Fermi hole' effects between parallel spin electrons exactly [5]. Of course, the HF method, according to Löwdin's definition [6], has no correlation energy. Therefore, having established the immediate merits of HF theory for the ground-state conformer of glycine in section 2 below, we consider in section 3 the changes brought about in the HF optimized nuclear geometry by adding second-order Møller–Plesset perturbation (MP2) corrections to the energy [7]. We bring these predictions of nuclear geometry of glycine in its ground-state into contact with experiment, and find fairly good accord. Therefore, we have next recalculated the HF electron density at the MP2 predicted geometry and exhibited specimen equidensity contours. Section 4 then focuses attention on the other quantities of central importance in DFT, namely exchange energy density and exchange potential. To be definite, we have singled out the Becke one-parameter exchange-energy density [8] by way of illustration. Section 5 consists of a summary, plus some suggestions for further work which should prove fruitful.

2. Ground-state conformer of glycine using HF theory

For the reasons set out above, we have used HF theory to treat the exchange effects between parallel spin electrons exactly. But, of course, we want to find the global minimum on the potential energy surface of glycine.

2.1. *Prelimilergy orientation*

Running a HF program with basis set 6-31G included in the programme Gaussian 03 to obtain a preliminary orientation, we found the optimized structure shown in figure 1. Evidently, this figure reflects the zwitterion structure referred to in the Abstract, with NH_3 and COO groups prominent. Since earlier workers [3,4] stress that the lowest conformer is of the non-ionized form NH_2–CH_2–COOH we shall merely summarize a few basic points arising from figure 1. First, and of major importance for the merits of HF theory as a starting point for treating glycine, the 5 non-hydrogenic nuclei lie, to high numerical accuracy in a plane. Second, the prominent C–N bond has predicted length 1.511 Å, to be compared with the experimental value 1.467 Å quoted in ref. [3]. Third, the total HF energy of the conformer displayed in figure 1 is −282.657 a.u.

However, because of the zwitterionic nature of the configuration depicted in figure 1, we have done more extensive calculations which reveal that figure 1 is a local, not a global, minimum, in HF theory.

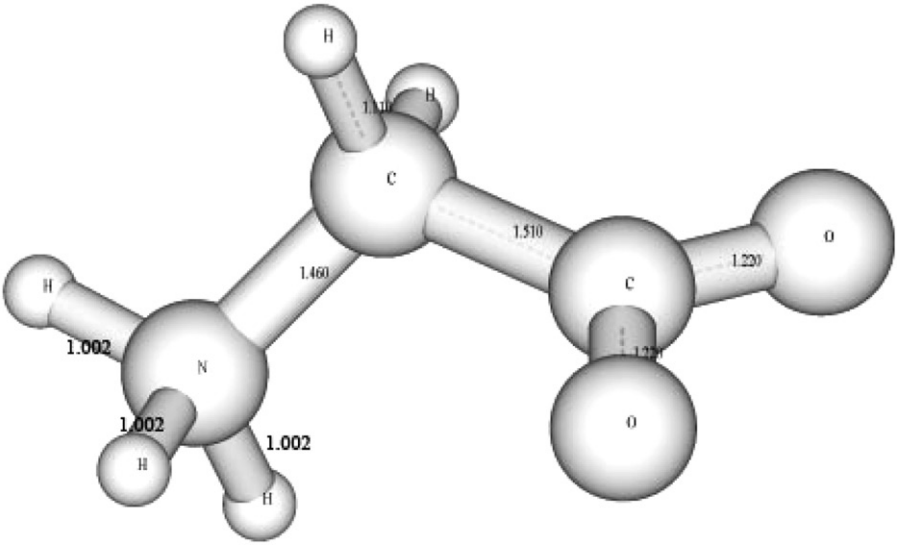

Figure 1. Preliminary orientation: optimized HF geometry and energy for glycine. Bond lengths are recorded on figure.

2.2. *Convergence on to global HF minimum of non-ionized form NH_2–CH_2–COOH*

Using the Aug-cc-p VTZ basis as implemented in Gaussian 03 the geometry of the global minimum of glycine was optimized.

Again, the heavy non-hydrogenic nuclei are accurately in a plane. The total HF energy is −282.955 a.u. This conformer is depicted in figure 2. The C–N bond length in this conformation is 1.4353 Å.

3. Changes brought about by addition of MP2 corrections

Let us again first consider the changes in figure 1 due to the addition of MP2 corrections. To gain orientation once more, we show in figure 3 a new optimized geometry energy from the MP2 perturbation energy being added to figure 1. The result is seen to be rather dramatic: we now have CH_2 and NH_2 groups rather than the zwitterion-like form in figure 1. But, because of such major changes in geometry, we can hardly expect low-order perturbation theory to be adequate. So we turn to deal, more thoroughly, with MP2 corrections applied to the non-ionized form shown in figure 2.

The main differences between the HF and MP2-corrected geometries for the global minimum are that bonds lengthen while valence angles are found to decrease. For bond lengths largest changes are found for both CO bonds which lengthen approximately 0.027 Å. The OH bond lengthening amounts to 0.024 Å.

For the valence angles largest changes are found for the COH valence angle which reduces from 108.96° (HF) to 106.16° (MP2). Other important changes are related to the NH valence angles: CNH reduces upon introduction of the MP2 corrections from 111.19° (HF) to 109.71° (MP2).

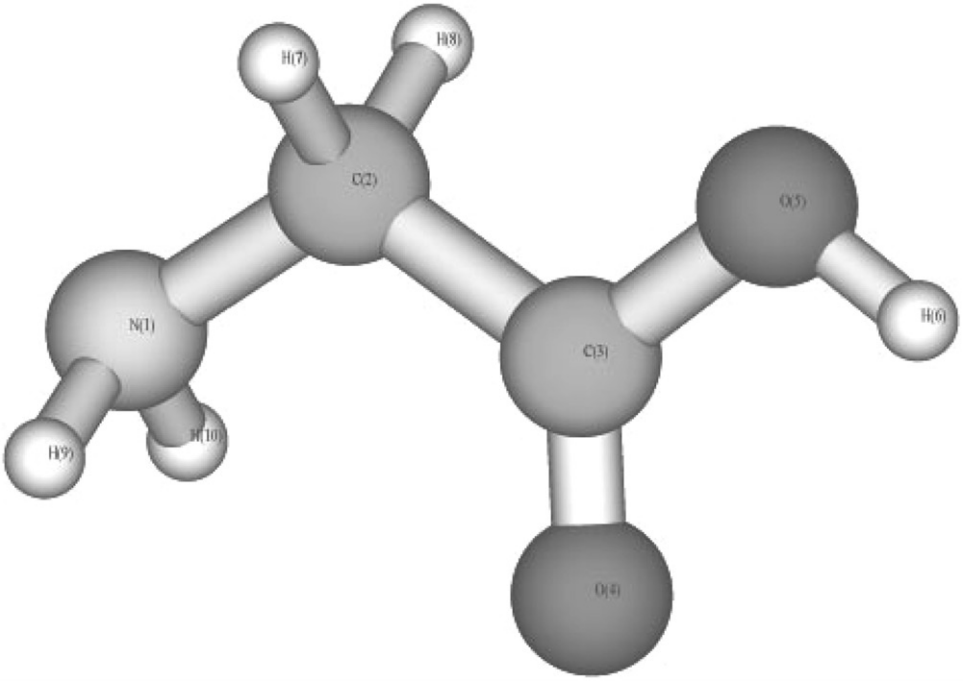

Figure 2. Global HF optimized geometry. Note that in contrast to figure 1 this is of form NH_2–CH_2–COOH.

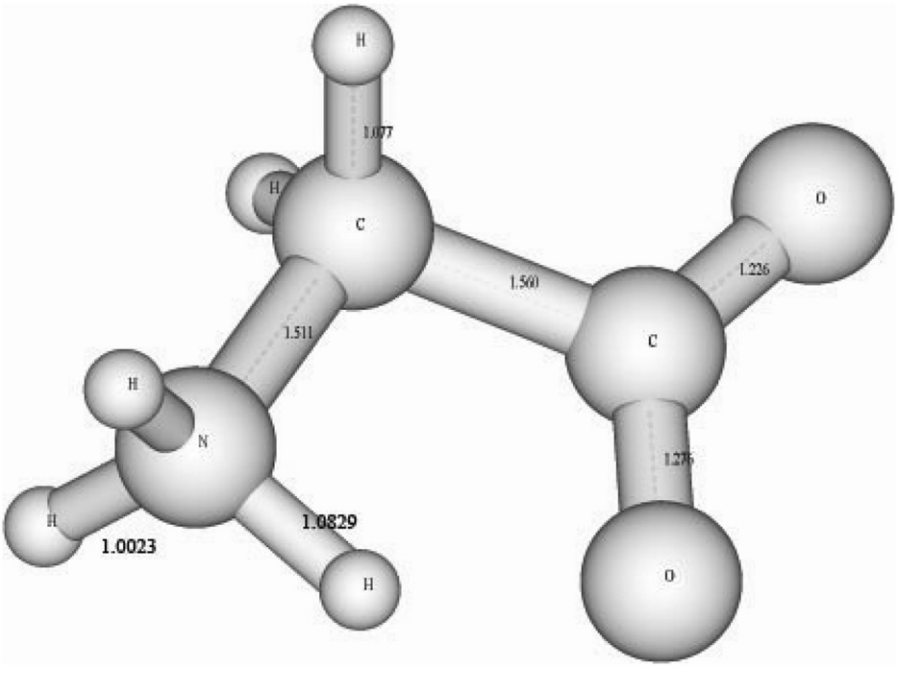

Figure 3. MP2 geometry starting from 'unperturbed' geometry in figure 1. Bond lengths are recorded on figure.

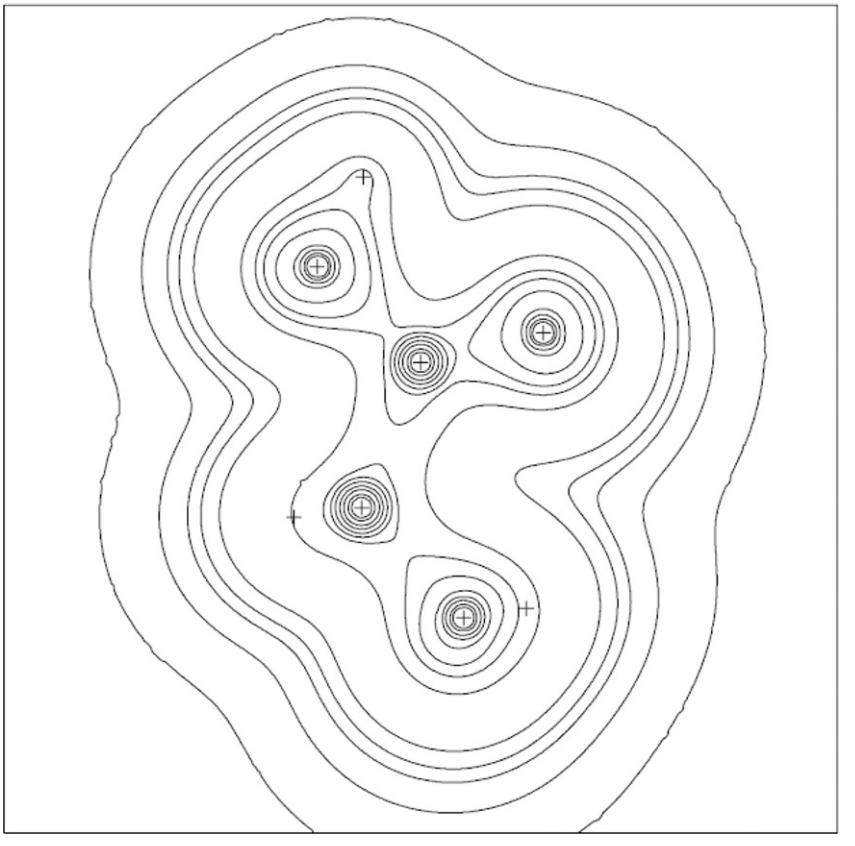

Figure 4. Equidensity $\rho(\boldsymbol{r})$ contours for glycine. The contour lines are drawn at values of 100, 50, 20, 10, 5, 3, 2, 1, 0.1, 0.05, 0.03, 0.01 and 0.001 e/Å^3, respectively.

In the light of the MP2 optimized geometry displayed in figure 2, we have recalculated the HF electron density with this nuclear framework. As use will be made of this refined density $\rho(\boldsymbol{r})$ in the following section in relation to approximations to exchange-energy density and exchange potential, in figure 4 we display in the plane containing the five heavy nuclei in glycine equidensity contours.

Two other low-lying conformers are recorded in Appendix 1.

4. Equiexchange-energy density contours for lowest conformer of glycine, from HF density matrix

In HF theory, we shall write the total exchange energy E_x as the volume integral of a density $\varepsilon_x(\boldsymbol{r})$:

$$E_x = \int \varepsilon_x \mathrm{d}\boldsymbol{r}. \tag{1}$$

While equation (1) does not suffice to define $\varepsilon_x(\boldsymbol{r})$ uniquely, it is natural to go back to the expression given by Dirac [5], which is valid for a single determinantal wave function (e.g. HF):

$$E_x = -\frac{1}{4}\int \frac{\gamma^2(\boldsymbol{r},\boldsymbol{r}')}{|\boldsymbol{r}-\boldsymbol{r}'|}\mathrm{d}\boldsymbol{r}\mathrm{d}\boldsymbol{r}' \tag{2}$$

and to then define $\epsilon_x(\boldsymbol{r})$ by

$$\varepsilon_x(r) = -\frac{1}{4}\int \frac{\gamma^2(\boldsymbol{r},\boldsymbol{r}')}{|\boldsymbol{r}-\boldsymbol{r}'|}\mathrm{d}\boldsymbol{r}'. \tag{3}$$

Here $\gamma(\boldsymbol{r},\boldsymbol{r}')$, is the Dirac density matrix, defined in the present context as

$$\gamma(\boldsymbol{r},\boldsymbol{r}') = 2\sum_{\substack{\text{occupied}\\ i}} \psi_i(\boldsymbol{r})\psi_i^*(\boldsymbol{r}') \tag{4}$$

where $\psi_i(\boldsymbol{r})$ denote the HF orbitals. As indicated explicitly in equation (4), the sum is restricted to occupied HF orbitals only.

Then, Slater [9] proposed intuitively, largely by analogy with electrostatics, that an exchange potential, which we denote by $V_x^{Sl}(\boldsymbol{r})$ below, should satisfy

$$E_x = \frac{1}{2}\int \rho(\boldsymbol{r})V_x^{Sl}(\boldsymbol{r})\mathrm{d}\boldsymbol{r}. \tag{5}$$

Comparison with equation (2) suggests that one should identify $V_x^{Sl}(\boldsymbol{r})$ as

$$V_x^{Sl}(\boldsymbol{r}) = -\frac{1}{2\rho(\boldsymbol{r})}\int \frac{\gamma^2(\boldsymbol{r},\boldsymbol{r}')}{|\boldsymbol{r}-\boldsymbol{r}'|}\mathrm{d}\boldsymbol{r}' \tag{6}$$

where $\rho(\boldsymbol{r}) = \gamma(\boldsymbol{r},\boldsymbol{r}')|\,\boldsymbol{r}'=\boldsymbol{r}$. This equation (6) is Slater's proposed approximation for the exchange potential. Comparing equations (3) and (6), one is led immediately to the direct connection between the exchange energy density $\varepsilon_x(\boldsymbol{r})$ and the Slater exchange potential $V_x^{Sl}(\boldsymbol{r})$ as

$$V_x^{Sl}(\boldsymbol{r}) = \frac{2\varepsilon_x(\boldsymbol{r})}{\rho(\boldsymbol{r})}, \tag{7}$$

Kleinman [10] has strongly argued the merits of the approximate form (7), or its equivalent (6). Whereas the 'correct' exchange-only potential is defined by the functional derivative

$$\boldsymbol{V}_x(\boldsymbol{r}) = \frac{\delta \boldsymbol{E}_x}{\delta\rho(\boldsymbol{r})}, \tag{8}$$

Kleinman pointed out that the Slater potential is a partial functional derivative of E_x in equation (2). Kleinman's study was formally completed by Holas and March [11], who exhibited the 'correction' terms to add to $V_x^{Sl}(\boldsymbol{r})$ to give $V_x(\boldsymbol{r})$ in equation (8), but no practical calculations by their route have, to our knowledge, been carried out to date.

Following this background, we turn now to the approximate exchange energy density functional $E_x[\rho]$ proposed by Becke [8]. Whereas $\varepsilon_x(\boldsymbol{r})$ involves the Dirac density matrix

$\gamma(\boldsymbol{r},\boldsymbol{r}')$ through equation (3), Becke corrects the local density approximation (LDA) proportional to $\rho(\boldsymbol{r})^{3/4}$ by writing [8],

$$\varepsilon_x(\boldsymbol{r}) = \varepsilon_x^{LDA}(\boldsymbol{r}) - \frac{\beta}{2^{1/3}}\rho(\boldsymbol{r})^{4/3}\frac{\{x(\boldsymbol{r})\}^2}{1+6\beta x(\boldsymbol{r})\sinh^{-1}x(\boldsymbol{r})} \tag{9}$$

where $x(\boldsymbol{r})$ is defined by

$$x(\boldsymbol{r}) = 2^{1/3}\frac{|\nabla_r\rho(\boldsymbol{r})|}{\rho(\boldsymbol{r})^{4/3}} \tag{10}$$

while β is the Becke parameter with recommended value $\beta = 0042.0$ atomic units. $\varepsilon_x^{\mathrm{LDA}}(\boldsymbol{r})$ in equation (9) is given explicitly by

$$\varepsilon_x^{\mathrm{LDA}}(\boldsymbol{r}) = -c_x\rho(\boldsymbol{r})^{4/3} : c_x = \frac{3}{4}e^2\left(\frac{3}{\pi}\right)^{1/3}. \tag{11}$$

We turn next to illustrate briefly the quantitative applicability of the Becke form (9) on a one-centre example, where both $\rho(\boldsymbol{r})$ and $\varepsilon_x(\boldsymbol{r})$ have been calculated in exact analytical form.

4.1. Accuracy of the Becke form (9) on a 10-electron non-relativistic atomic ion in the limit of large atomic number Z

From the so-called 1/Z expansion which is a pillar of atomic theory [12], as the atomic number Z becomes sufficiently large, $\rho(\boldsymbol{r})$ can be approximated by pure Coulomb wave functions. Then March and Santamaria [13] find $\rho(\boldsymbol{r})$ to be exactly, for filled K plus L shells,

$$\begin{aligned}\rho(r) = {} & \left(\frac{2}{\pi}\right)\left(\frac{\mathrm{Z}}{a_0}\right)^3\exp\left(\frac{-2Zr}{a_0}\right) \\ & + \left(\frac{1}{4}\pi\right)\left(\frac{\mathrm{Z}}{a_0}\right)^3\exp\left(\frac{-Zr}{a_0}\right)\left[\frac{1-Zr}{a_0}+\frac{1}{2}\left(\frac{Zr}{a_0}\right)^2\right] \\ & : a_0 = \frac{\hbar^2}{me^2} = 1 \text{ a.u.}\end{aligned} \tag{12}$$

These authors also gave the Dirac density matrix $\gamma(\boldsymbol{r},\boldsymbol{r}')$ in closed form, which is such that $\gamma(\boldsymbol{r},\boldsymbol{r}')|_{\boldsymbol{r}'=\boldsymbol{r}} = \rho(\boldsymbol{r})$ in equation (12). Subsequently, Howard *et al.* [14] utilized this pure Coulomb density matrix γ in equation (4) to calculate $\epsilon_x(\boldsymbol{r})$ exactly as

$$\begin{aligned}\varepsilon_x(\boldsymbol{r}) = {} & (1/15552)\left(\frac{e^2\alpha^3}{\pi\boldsymbol{r}}\right)\exp(-4\alpha\boldsymbol{r}) \\ & \{15552(1+\alpha\boldsymbol{r}) + \exp(\alpha r)[4096+3840(\alpha\boldsymbol{r})+2304(\alpha\boldsymbol{r})^2+3456(\alpha\boldsymbol{r})^3] \\ & + \exp(2\alpha\boldsymbol{r})\begin{bmatrix}-13068+2430(\alpha\boldsymbol{r})+2916(\alpha\boldsymbol{r})+2916(\alpha\boldsymbol{r})^2\\ +1944(\alpha\boldsymbol{r})^3+486(\alpha\boldsymbol{r})^4+243(\alpha\boldsymbol{r})^5\end{bmatrix} \\ & -4096\exp\left(\frac{5\alpha\boldsymbol{r}}{2}\right)+\exp(3\alpha\boldsymbol{r})[-1944-972\alpha\boldsymbol{r}-972(\alpha\boldsymbol{r})^5]\} \\ & \text{where } \alpha = \frac{Z}{a_0} = Z \text{ a.u.}\end{aligned} \tag{13}$$

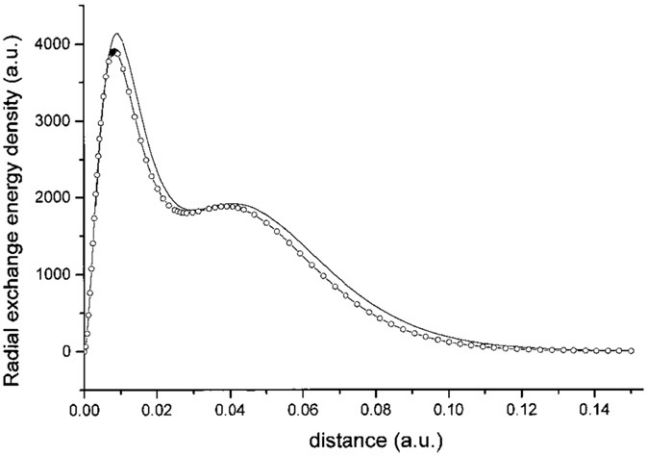

Figure 5. $4\pi r^2\epsilon_x(\boldsymbol{r})$ *vs.* r in atomic units ($e^2=1$, $a_0=1$). Upper curve was obtained using formula (13) with z = 92. Lower curve is IDA in equation (11), using exact density in equation (12). While the integrated difference in total exchange energy E_x is 13 a.u., Becke's formula (9) reduces the discrepancy to ~ 0.2 a.u. [redrawn from [14]].

For Z = 92, the so-called radial exchange energy density $4\pi r^2\varepsilon_x(\boldsymbol{r})$ is compared, using the exact form (13), with the approximation (11), this being calculated with the exact density $\rho(\boldsymbol{r})$ in equation. (12). These two results are reproduced in figure 5, and the agreement to graphical accuracy is somewhat remarkable for the simplicity of the LDA form. However, there is still a significant difference between the areas under the two curves, the exact exchange energy E_x being given by

$$E_x(\mathrm{Z}) = -1.74788\mathrm{Z}\frac{e^2}{a_0}$$
$$: a_0 = \frac{h^2}{me^2} = 1 \text{ a.u.} \tag{14}$$

the value being $E_x = -160.805$ a.u. for Z = 92, of which LDA in equation (11) contributes -147.969 a.u. The accuracy of Becke's formula, mentioned explicitly in section 4.2 below, greatly reduces this difference, leaving a discrepancy of about 0.2 a.u.

With this brief introduction using an analytic atomic example, let us return to the HF density matrix $\gamma(\boldsymbol{r},\boldsymbol{r}')$ for the lowest conformer of glycine and to use this matrix to calculate $\varepsilon_x(\boldsymbol{r})$ from equation (3). The details of how this has been achieved are recorded in an Appendix. We turn to present equiexchange-energy density contours for glycine.

4.2. *Contours of constant exchange energy density $\varepsilon_x(r)$ for glycine*

Figure 6 shows the results of the above calculations. Comparison with the equielectron HF density contours in figure 4 shows, at first sight, some considerable similarity of shape. While this might appear to vindicate the LDA exchange for the HF theory of glycine, appeal to the earlier example of an atomic ion in LDA warns of a major error in the total exchange energy. Such an error would, of course be unacceptable for glycine. From the exchange energy density $\varepsilon_x(\boldsymbol{r})$ displayed in figure 6 we find the

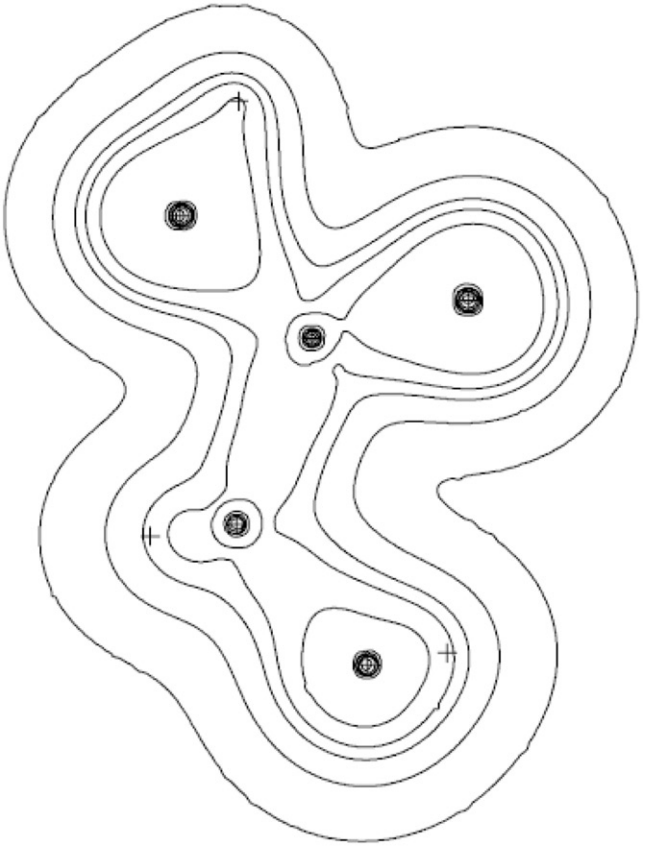

Figure 6. Contours of constant exchange energy density $\varepsilon_x(\boldsymbol{r})$ for lowest conformer of glycine in plane of five heavy nuclei. This was calculated from the HF density matrix $\gamma(\boldsymbol{r},\boldsymbol{r}')$ via equation (3). Contour values are the same as those for figure 2, however now units are a.u.

total HF exchange energy for glycine to be $\varepsilon_x = -8.09418$ a.u. The accuracy of Becke's one-parameter exchange discussed above, of $\approx 0.1\%$, is still a sigificant error by chemical standards relevant to biologically important molecules such as glycine.

Nevertheless, because of the practicability of DFT for even much larger amino acids, we shall conclude this section by giving results for the non-local Slater exchange potential defined in equation (7) above.

4.3. *Contours of equipotential for Slater's exchange potential* $V_x^{Sl}(\boldsymbol{r})$

From equation (7), we merely require twice the quotient of $\varepsilon_x(\boldsymbol{r})$ and $\rho(\boldsymbol{r})$, the HF quantities presented in figures 6 and 4, respectively.

The equipotential contours are displayed in figure 7, and we stress that $V_x^{Sl}(\boldsymbol{r})$ shown there represents a fundamentally non-local approximation. It seems clear that departures from locality are more substantial for the exchange potential than for the exchange energy density.

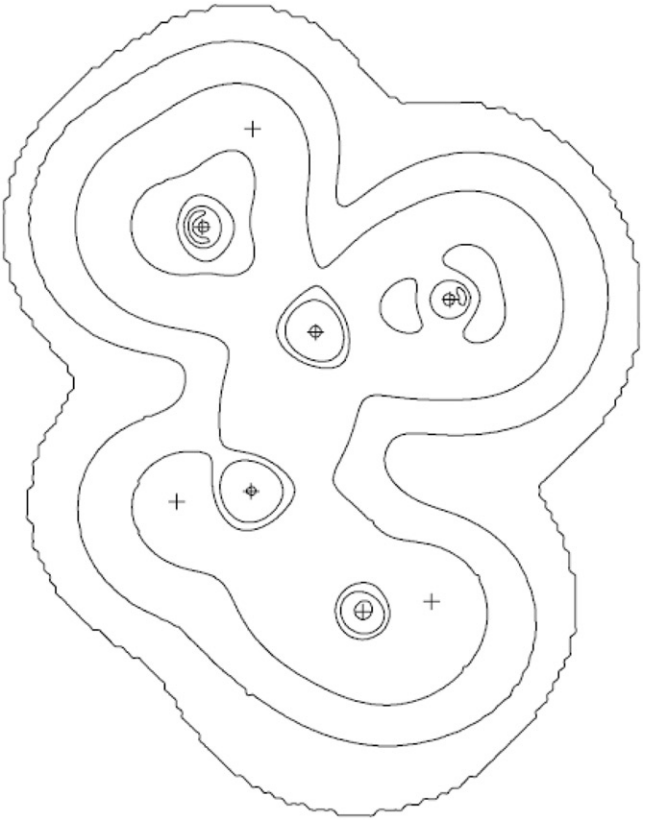

Figure 7. Slater's non-local exchange potential $V_x^{\text{Slater}}(\boldsymbol{r})$ calculated from equation (7) using $\varepsilon_x(\boldsymbol{r})$ and $\rho(\boldsymbol{r})$ from the HF results shown in figures 7 and 5, respectively.

5. Summary and proposed future directions

The main achievements of the present work are as follows:

(i) The calculation of the ground-state electron density $\rho(\boldsymbol{r})$ of the lowest conformer of glycine displayed in figure 4, by HF theory, but used at the optimized MP2 nuclear geometry.

(ii) The determination of the HF exchange energy density $\varepsilon_x(\boldsymbol{r})$ for the same geometry from the HF first-order density matrix $\gamma(\boldsymbol{r}, \boldsymbol{r}')$. The shapes of the equiexchange energy density contours in figure 6 do reflect quite well the $\rho(\boldsymbol{r})$ equidensity contours in the present HF theory of glycine. However, it is of obvious importance in molecules of biological interest to get truly quantitative exchange energies, such as we have obtained here for the ground state conformer of glycine.

We want finally to point some further directions which should prove fruitful. We have checked, in both HF theory and with HF + MP2 corrections that the structure of the lowest conformer presented has real vibrational frequencies. We believe it important for the future to assess the changes in (a) nuclear geometry of glycine and (b)

correlation energy, caused by MP4 additional corrections. Even at MP2, we can define a correlation energy density $\varepsilon_C^{MP2}(\boldsymbol{r})$ by

$$E_C^{MP2} = \int \varepsilon_C^{MP2}(\boldsymbol{r})\mathrm{d}\boldsymbol{r}. \tag{15}$$

In the future, it will be of interest to attempt to plot $\varepsilon_C^{MP2}(\boldsymbol{r})$ to examine whether again LDA for the correlation correction is a useful starting point for describing the HF + MP2 results for glycine. However, it has to be borne in mind now that while HF theory settles the question of the exchange-energy density $\varepsilon_x(\boldsymbol{r})$, and its volume integral E_x, the correlation correction E_C^{MP2} in equation (15) can only be a fraction of the total correlation energy, using Löwdin's definition. Naturally, to gain further insight into the departures from LDA of $\varepsilon_C^{MP2}(\boldsymbol{r})$ in equation (15) in glycine and other amino acids will be important for future DFT studies of really large molecules of biological interest.

Acknowledgements

N. H. March acknowledges that his contribution to this study was mainly carried out during a visit to DKFZ, Heidelberg. He thanks the Center for generous hospitality in the form of a scholarship. C. Van Alsenoy gratefully acknowledges the University of Antwerp for access to the university's computer cluster CalcUA. The authors would also like to thank Andrea McIntosh-Suhr for her help in preparing the manuscript.

References

[1] M. Wanko, M. Hoffmann, P. Strodel, A. Koslowski, W. Thiel, F. Neese, T. Frauenheim, M. Elstner. *J. Phys. Chem*, **109**, 3606 (2005).
[2] M. Knapp-Mohammady, K.J. Jalkanen, F. Nardi, R.C. Wade, S. Suhai. *Chem. Phys*, **240**, 63 (1999).
[3] S.G. Stepanian, I.D. Reva, E.D. Radchenko, Rosado, M.T.S. Duarte, , R. Fausto. *J. Phys. Chem. A*, **102**, 1041 (1998).
[4] W. Wang, Pu, X., W. Zheng, N. Wong, A. Tian. *Chem. Phys. Letts*, **370**, 147 (2003).
[5] R. McWeeny. *Methods of Molecular Quantum Mechanics*, Academic Press, London (1992).
[6] P. Löwdin. *O. Phys. Rev*, **97**, 1474 (1955).
[7] J.S. Binkley, J.A. Pople. *Int. J. Quantum Chem*. **9**, 229 (1975).
[8] A.D. Becke. *Phys. Rev. A*, **38**, 3098 (1988).
[9] J.C. Slater. *Phys. Rev*, **81**, 385 (1951).
[10] L. Kleinman. *Phys. Rev. B*, **49**, 14197 (1994).
[11] A. Holas, N.H. March. *Phys. Rev. B*, **55**, 1295 (1997).
[12] N.H. March, R.J. White, *J. Phys. B*, **5**, 466 (1972).
[13] N.H. March, R. Santamaria. *Phys. Rev. A*, **38**, 5002 (1988).
[14] I.A. Howard, N.H. March, P. Senet, V.E. Van Doren. *Phys. Rev. A*, **62**, 062512 (2000).
[15] M.J. Frisch, G.W. Trucks, H.B. Schlegel, G.E. Scuseria, M.A. Robb, V. Cheeseman, J.A. Montgomery, V. Vreven, K.N. Kudin, J.C. Burant, J.M. Millam, S.S. Iyengar, J. Tomasi, V. Barone, B. Mennucci, M. Cossi, V. Scalmani, V. Rega, G.A. Petersson, H. Nakatsuji, M. Hada, M. Ehara, K. Toyota, R. Fukuda, J. Hasegawa, M. Ishida, T. Nakajima, Y. Honda, O. Kitao, H. Nakai, M. Klene, X. Li, J.E. Knox, H.P. Hratchian, J.B. Cross, C. Adamo, J. Jaramillo, R. Gomperts, R.E. Stratmann, O. Yazyev, A.J. Austin, R. Cammi, C. Pomelli, J.W. Ochterski, P.Y. Ayala, K. Morokuma, G.A. Voth, P. Salvador, J.J. Dannenberg, V.G. Zakrzewski, S. Dapprich, A.D. Daniels, M.C. Strain, O. Farkas, D.K. Malick, A.D. Rabuck, K. Raghavachari, J.B. Foresman, J.V. Ortiz, Q. Cui, A.G. Baboul, S. Clifford, J. Cioslowski, B.B. Stefanov, G. Liu, A. Liashenko, P. Piskorz, I. Komaromi, R.L. Martin, D.J. Fox, T. Keith, M.A. Al-Laham, C.Y. Peng, A. Nanayakkara, M. Challacombe, P.M.W. Gill, B. Johnson, W. Chen, M.W. Wang, C. Gonzalez, J. A. Pople. Gaussian 03, Revision A.1, Gaussian, Inc., Pittsburgh PA (2003).

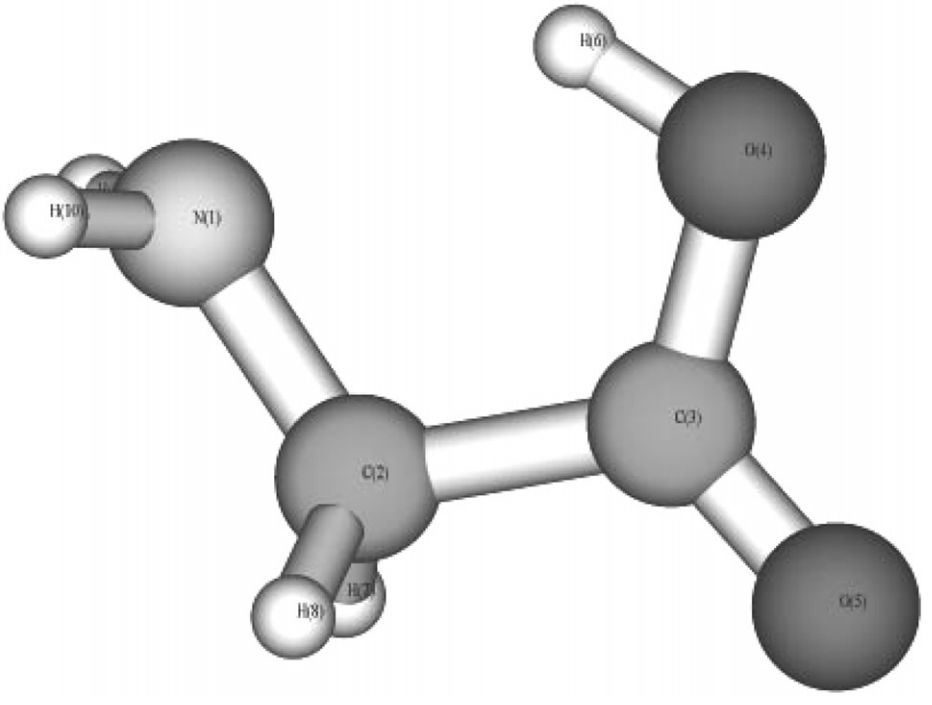

Figure A1.1. Low-lying conformers of glycine from HF theory, with energy above configuration in figure 2 by 2.86 kcal mol^{-1}.

Appendix 1

Two further low-lying glycine conformers

The global HF minimum has been illustrated in figures 2 and 4 of the main text. In this Appendix, we record structures (Figures A1.1 and A1.2) of two HF low-lying conformers corresponding to local minima on the glycine potential energy surface. Differences in geometry between these conformers is summarized in Table A1.

Appendix 2

Methodology for calculating exchange-energy density $\varepsilon_x(\vec{r})$ from HF first-order density matrix $\gamma(\vec{r},\vec{r}\,')$.

Hartree–Fock orbitals are used to evaluate the electron density $\rho(\boldsymbol{r})$ as well as the exchange density $\varepsilon_x(\vec{r})$ as defined in

$$\varepsilon_x(\vec{r}) = -\frac{e^2}{4}\sum_{i<j}\int \frac{\varphi_i(\vec{r}\,')\varphi_j(\vec{r}\,')}{|\vec{r}-\vec{r}\,'|}\mathrm{d}\boldsymbol{r}\,'\varphi_i(\vec{r})\varphi_j(\vec{r})$$

which is a realization of the Dirac density matrix in terms of HF-orbitals. For a given point $\boldsymbol{r}$, space in the integrals

$$\int \frac{\chi_\mu(\vec{r}\,')\chi_\nu(\vec{r}\,')}{|\vec{r}-\vec{r}\,'|}\mathrm{d}\boldsymbol{r}\,'$$

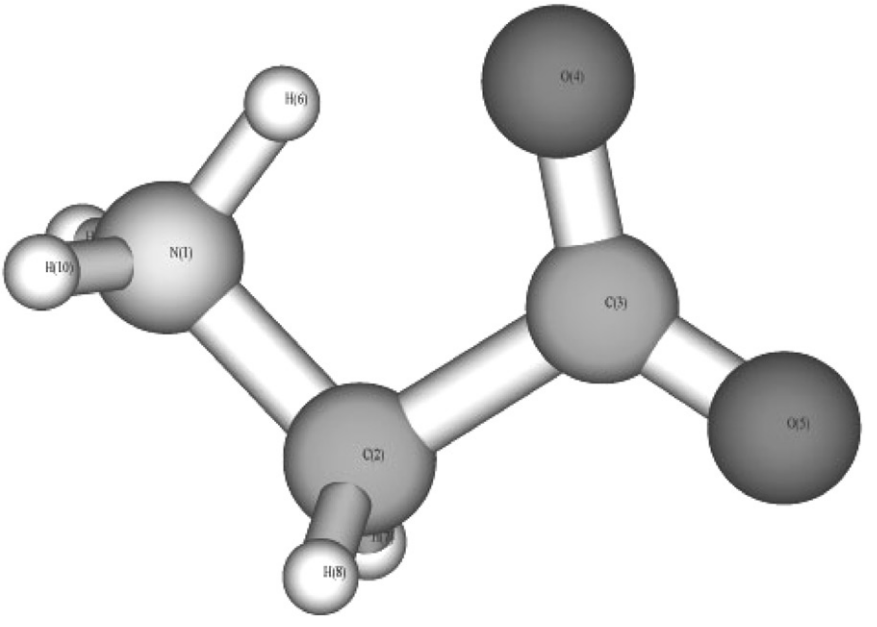

Figure A1.2. A further, slightly higher energy conformer for glycine than that shown in figures 2 by 3.12 kcal mol^{-1}.

Table A1. Differences in geometry between the conformers A1.1 and A1.2.

	A1.2	A1.1
C2–N1	1.4522	1.4523
C3–C2	1.5148	1.5226
O4–C3	1.2050	1.3201
O5–C3	1.1403	1.1735
H6–N1	1.0132	
H6–O4		0.9450
H7–C2	1.0215	1.0777
H8–C2	1.0274	1.0783
H9–N1	0.9326	0.9908
H10–N1	0.9246	0.9898
C3–C2 – N1	101.62	113.51
O4–C3–C2	111.45	115.29
O5–C3–C2	114.59	121.80
O5–C3–O4	133.94	122.88
H6–N1–C2	99.31	
H6–O4–C3		108.07

are calculated over the atomic orbitals χ_μ and χ_ν: then transformed to the Molecular Orbital basis and subsequently multiplied with the values of the MO's $\varphi_i(\vec{r})$ and $\varphi_j(\vec{r})$ at position $\vec{r}$.